

# Constraints on the Transition Redshift using the Cosmic Triangle and Hubble Phase Space Portrait

Darshan Kumar<sup>1</sup>★, Deepak Jain<sup>2</sup>†, Shobhit Mahajan<sup>1</sup>‡, Amitabha Mukherjee<sup>1</sup>§ and Akshay Rana<sup>3</sup>¶

<sup>1</sup>Department of Physics and Astrophysics, University of Delhi, Delhi 110007, India

<sup>2</sup>Deen Dayal Upadhyaya College, University of Delhi, Dwarka, New Delhi 110078, India

<sup>3</sup>St. Stephen's College, University of Delhi, Delhi 110007, India

Accepted XXX. Received YYY; in original form ZZZ

## ABSTRACT

One of the most significant discoveries in modern cosmology is that the universe is currently in a phase of accelerated expansion after a switch from a decelerated expansion. The redshift corresponding to this time is commonly referred as the transition redshift  $z_t$ . In this work we put constraints on the transition redshift with both model-dependent and model-independent approaches. We consider the recently compiled database of 32 Hubble parameter measurements. In order to include the possible systematic effects in this analysis, we use full covariance matrix of systematic uncertainties. In the first part we follow a model dependent approach. Here, we consider a non-flat  $\Lambda$ CDM model as a background cosmological model. Further we reconstruct cosmic triangle plot among  $\log(\Omega_{m0})$ ,  $-\log(2\Omega_{\Lambda0})$  and  $3\log(1+z_t)$  where the constraints of each parameter are determined by the location in this triangle plot. Using  $\Omega_{m0}$  and  $\Omega_{\Lambda0}$  values, we find the best value of the transition redshift  $z_t = 0.619^{+0.580}_{-0.758}$ , which is in good agreement with the Planck 2018 results at  $1\sigma$  confidence level. The second part is based on a non-parametric method. We plot a Hubble Phase Space Portrait (HPSP) between  $\dot{H}(z)$  and  $H(z)$ . From this HPSP diagram, we estimate the transition redshift as well as the current value of the equation of state parameter  $\omega_0$  in a model-independent way. We find the best fit value of  $z_t = 0.591^{+0.365}_{-0.365}$  and  $\omega_0 = -0.677^{+0.284}_{-0.284}$ . We also simulate the observed Hubble parameter measurements in the redshift range  $0 < z < 2$  and perform the same analysis to estimate the transition redshift.

**Key words:** Cosmological Parameters: matter density–curvature density–transition redshift–equation of state, Observational dataset: Hubble parameter, Methods: Chi-square–Gaussian process

## 1 INTRODUCTION

It is now widely believed that we live in a phase of accelerated expansion of the universe, which has been corroborated by several independent observations. The most direct and obvious evidence of the present accelerating stage of the universe comes from the luminosity distance versus redshift relation measurements using Type Ia supernovae (SNe Type Ia) which are confirmed by two different research groups Riess et al. (1998); Perlmutter et al. (1999). Over the decades, the number of SNe Type Ia catalogues have grown substantially. Even now, the SNe Type Ia observations provide the most direct evidence for the current cosmic acceleration

(Astier et al. (2006); Riess et al. (2007); Davis et al. (2007); Kowalski et al. (2008); Amanullah et al. (2010); Suzuki et al. (2012); Goobar et al. (2018)). This discovery is also supported by complementary observations such as the Cosmic Microwave Background (CMB) radiation measurements (Komatsu et al. (2011); Larson et al. (2011); Planck Collaboration et al. (2020)), Baryonic Acoustic Oscillations (BAO) measurements (Eisenstein et al. (2005); Percival et al. (2007); Eisenstein et al. (2011); Dawson et al. (2013); Cuceu et al. (2019)) and Hubble parameter ( $H(z)$ ) measurements (Stern et al. (2010); Farooq et al. (2013b); Farooq & Ratra (2013); Moresco (2015); Moresco et al. (2016); Farooq et al. (2017)). From a theoretical point of view, the simplest and most popular  $\Lambda$ CDM model supports such an accelerating phase, with free parameters being tightly constrained by Planck Collaboration et al. (2020). In the standard model of cosmology, there was an era of decelerated expansion due to non-relativistic (cold dark and baryonic) matter dominated universe (Ratra & Vogeley (2008); Martin (2012); Huterer & Shafer (2018)).

★ E-mail: darshanbeniwal11@gmail.com

† E-mail: djain@ddu.du.ac.in

‡ E-mail: sm@physics.du.ac.in

§ E-mail: am@physics.du.ac.in

¶ E-mail: akshay@ststephens.edu

Given the transition from a decelerated to an accelerated expansion of the universe, it is important to precisely determine the redshift at which the universe started to accelerate from a decelerated phase. The parameter corresponding to such a transition from decelerated to an accelerated phase is referred to as the transition redshift  $z_t$  and it may be treated as a new cosmic parameter along with the present deceleration parameter  $q_0$  and the Hubble constant  $H_0$ . It is now commonly accepted that the upper bound on the transition redshift is less than unity, which has been confirmed by multiple independent investigations in both model-dependent and model-independent approaches (Farooq et al. (2013b); Farooq & Ratra (2013); Sharov & Vorontsova (2014); Shapiro & Turner (2006); Cunha & Lima (2008); Rani et al. (2015); Lima et al. (2012); Moresco et al. (2016); Jesus et al. (2018); Velasquez-Toribio & Maganao (2020)). Shapiro & Turner (2006) in their analysis adopted a model-dependent approach and using SNe Type Ia observations, they put a constraint on the deceleration parameter  $q(z)$  and transition redshift  $z_t$ . By considering different dynamical dark energy models, Melchiorri et al. (2007) put constraints on  $z_t$ . Similarly, Rapetti et al. (2007) developed a new kinematic method to estimate  $z_t$  using the measurements of X-ray cluster gas mass fraction. On the other hand, people also have studied the transition redshift in modified gravity models (Capozziello et al. (2015)).

Further, by considering the dynamical nature of  $q(z)$ , authors have explored constraints on the transition redshift. For example, Cunha & Lima (2008) have used a linear parametrization of the deceleration parameter i.e.  $q(z) = q_0 + q_1 z$ . In their work, the value of transition redshift is  $z_t = 0.43^{+0.09}_{-0.05}$  which was obtained by using 182 SNe Type Ia (Riess et al. (2007)). By using the SNLS data set, Astier et al. (2006) find the value to be  $z_t = 0.61^{+3.68}_{-0.21}$ . Rani et al. (2015) also used the linear parametrization of the deceleration parameter and by using a joint analysis of age of galaxies, strong gravitational lensing and SNe Ia data, they found  $z_t \approx 0.98$ . Along the same lines, other researchers have updated the study by introducing additional data sets and modifying the parametrizations for  $q(z)$ . For the parametrization  $q(z) = q_0 + q_1 z / (1 + z)$  and using 307 SNe Type Ia together with BAO and  $H(z)$  data, Xu et al. (2009) found  $z_t = 0.609^{+0.110}_{-0.070}$ . This type of parametrization has also been investigated by Elgarøy & Multmäki (2006). Using different datasets such as Gamma Ray Bursts (GRBs), Hubble Observational Data  $H(z)$ , BAO, CMB, Galaxy Clusters, lookback time etc., many authors have reconstructed the deceleration parameter and put constraints on the transition redshift (Nair et al. (2012); Wang & Dai (2006); Xu et al. (2009); Cunha & Lima (2008); Gong & Wang (2007); Lima et al. (2009); Farooq et al. (2013a); Farooq & Ratra (2013); Riess et al. (2004); Cai & Tuo (2011); Vargas dos Santos et al. (2016)). These authors, along with the aforementioned two parametrizations for  $q(z)$ , have considered different types of parametrizations. Recently, by considering  $\Lambda$ CDM model as a background cosmological model, Planck Collaboration et al. (2020) put a constraint on the transition redshift  $z_t = 0.632 \pm 0.018$ .

The determination of the deceleration parameter  $q$  and hence transition redshift  $z_t$ , as one may see, is an important and relevant subject in modern cosmology along with the determination of the current value of Hubble parameter  $H_0$ . The determination of these parameters plays a vital role in the understanding of the universe. An alternate and innovative approach for accessing cosmic parameters is a model-independent one by means of the study of Hubble parameter estimated from the Cosmic Chronometers (CC) approach.

In the literature, an even more intriguing statistical technique of obtaining cosmic parameters has been developed by Seikel et al.

(2012). This method is called Gaussian Process (GP). In cosmology, using such statistical and non-parametric method, one can reconstruct a redshift dependent cosmological function such as the expansion rate, luminosity distance etc. Using cosmological observations corresponding to these functions, one can put constraints on different cosmological parameters. By adopting this model-independent approach, Jesus et al. (2020) found the transition redshift as  $z_t = 0.59^{+0.12}_{-0.11}$  from  $H(z)$  measurements. On the other hand, using the recent and largest up-to-date Pantheon compilation of SNe Type Ia, Scolnic et al. (2018) obtained  $z_t = 0.683^{+0.110}_{-0.082}$  in a non-parametric way. Further, using the GP approach, the analysis of Lin et al. (2019) yields  $z_t = 0.59^{+0.05}_{-0.05}$ . In their analysis, they reconstructed the equation of state of dark energy and cosmic expansion using Gaussian Process from the Pantheon data and  $H(z)$ .

In the present work we use updated Hubble parameter measurements and obtain the transition redshift in both a model-dependent and model-independent way. This work is divided into two parts. In the first part we carry out the analysis in a **model-dependent way**. We consider a non-flat  $\Lambda$ CDM model as a background cosmological model and after marginalization over  $H_0$  using a uniform prior, we put constraints on the cosmological density parameters i.e.  $\Omega_{m0}$ ,  $\Omega_{k0}$ , and  $\Omega_{\Lambda0}$ . Using the sum rule of these three cosmological density parameters i.e.  $\Omega_{m0} + \Omega_{k0} + \Omega_{\Lambda0} = 1$ , we represent them by an equilateral triangle and the so-called ternary plot, where, each parameter runs parallel to each of the edges on the equilateral triangle. The sum rule must be satisfied at every location where lines of constant  $\Omega_{m0}$ ,  $\Omega_{k0}$ , and  $\Omega_{\Lambda0}$  intersect. This is similar to the ‘cosmic triangle’ described by Bahcall et al. (1999). Further, using a relation between  $z_t$ ,  $\Omega_{m0}$  and  $\Omega_{\Lambda0}$ , we update the ternary plot and estimate the transition redshift. We also adopt a **model-independent** approach in the second part of this work. With the help of Gaussian Process, we reconstruct the Hubble parameter  $H(z)$  and its time-derivative  $\dot{H}(t)$  from Hubble parameter measurements. We plot a diagram between  $\dot{H}(z)$  versus  $H(z)$  which is generally referred to as the Hubble Phase Space Portrait (HPSP). By analysing this diagram, we put constraints on  $z_t$  as well as on the present value of the equation of state parameter  $\omega_0$ . By introducing the updated cosmic triangle plot and Hubble Phase Space Portraits, we propose that these representations will help to visualise and estimate the parameters in a unique way. We also simulate the observed Hubble parameter measurements in the redshift range  $0 < z < 2$  to estimate the transition redshift.

The outline of the paper is as follows. In section 2, we discuss the Hubble parameter measurements and tabulate the new  $H(z)$  data. Section 3 introduces the background of ‘Cosmic Triangle’, ‘Hubble Phase Space Portrait’ and the methodology used to obtain the constraints on the transition redshift. In section 4, we discuss the results. Finally, we summarize the conclusions in Section 5.

## 2 HUBBLE PARAMETER MEASUREMENTS

The Hubble parameter  $H(z)$  which addresses the dynamical features of the universe like its expansion rate and evolution history is a crucial quantity in cosmology. It is also useful to investigate the nature of the dark energy since this parameter can be inferred directly from astrophysical observations which do not depend on any underlying cosmological model. There are other probes which do not directly measure  $H(z)$ , but rather integrated quantities such as luminosity distances. Currently, the most common methods for obtaining  $H(z)$  data are (i) using the differential ages of passively evolving galaxies, generally referred to as ‘Cosmic Chronometers

(CC)' (Jimenez et al. (2003); Simon et al. (2005)) (ii) measurements of peaks of acoustic oscillations of baryons (BAO) (Eisenstein et al. (2005); Percival et al. (2007); Gaztañaga et al. (2009); Bassett & Hlozek (2010); Benítez et al. (2009)) (iii) Redshift Drift (Sandage (1962); McVittie (1962)).

In this work, we consider the  $H(z)$  measurements obtained by using Cosmic Chronometers. The Hubble parameter  $H(z)$  in terms of redshift  $z$  can be expressed as

$$H(z) = -\frac{1}{1+z} \frac{dz}{dt} \quad (1)$$

However, when employing this approach to calculate  $H(z)$ , significant caution must be exercised in the selection of galaxies. Stars are continually born in early developing galaxies and the emission spectra will be dominated by the young stellar population. As a result, passively developing red galaxies are utilised to properly estimate the differential ageing of the universe since their light is dominated by the elderly star population (Jimenez et al. (2003)). For measurements of  $H(z)$ , the term  $dt$  is to be estimated using the differential age evolution of the universe in a given interval of redshift  $dz$ . For the estimation of  $dt$ , Moresco et al. (2012) suggested the use of a direct spectroscopic observable (4000Å break) which is known to be linearly related to the age of the stellar population of a galaxy at fixed metallicity. Thus, the measurement of  $H(z)$  is purely by using spectroscopic observations, is independent of the cosmological model and has proved to be a strong probe to constrain cosmological models and assumptions. The most recent data compilation of Hubble parameter measurements by Magaña et al. (2018) has 31 measurements of  $H(z)$  which are obtained by using the differential ages of passively evolving galaxies. Here we have added one additional datapoint complied by Borghi et al. (2022) at  $z = 0.75$ . Thus 32  $H(z)$  measurements used in this analysis are listed in Table 1, spanning the redshift range  $0.07 \leq z \leq 1.965$ .

## 3 BACKGROUND AND METHODOLOGY

### 3.1 The Cosmic Triangle

A triangle or ternary diagram is a graphical depiction of systems via an equilateral triangle having three-components which sum to a constant. A ternary diagram has some significant advantages over other graphical representations where the actual distribution of three-components is displayed as points within an equilateral triangle. The obvious advantage of this representation is that by presenting the three-variable data in a two-dimensional plot, it is easy to analyze the correlation among the three-variables simultaneously. Using a ternary diagram, Bahcall et al. (1999) proposed the 'cosmic triangle' to visualize the cosmological parameters. In this cosmic triangle they plotted the matter, curvature and cosmological constant density parameters; all these density parameters are related to one another since they follow the sum rule i.e.  $\Omega_{m0} + \Omega_{k0} + \Omega_{\Lambda0} = 1$ . In their analysis, they showed that the constraints on the cosmological parameters using cosmic triangle representation preferred the (now standard) flat  $\Lambda$ CDM model.

For example, suppose we have a non-linear relation between any two components (say  $a$ ,  $b$  and  $ab$ ). By taking the logarithm of each component in the triad one can propose a ternary plot where, a linear relationship condition is satisfied through  $\log_{10}(a) + \log_{10}(b) - \log_{10}(ab) = 0$ . In this context, recently, Bernal et al. (2021) propose a new cosmic triangle to visualize cosmological parameters like  $H_0$ ,  $t_U$  (age of the universe).

**Table 1.** Most recent compilation of Hubble parameter measurements.

$z$	$H(z)^a$	Reference
0.07	$69.0 \pm 19.6$	Zhang et al. (2014)
0.09	$69.0 \pm 12.0$	Simon et al. (2005)
0.12	$68.6 \pm 26.2$	Zhang et al. (2014)
0.17	$83.0 \pm 8.0$	Simon et al. (2005)
0.179	$75.0 \pm 4.0$	Moresco et al. (2012)
0.199	$75.0 \pm 5.0$	Moresco et al. (2012)
0.2	$72.9 \pm 29.6$	Zhang et al. (2014)
0.27	$77.0 \pm 14.0$	Simon et al. (2005)
0.28	$88.8 \pm 36.6$	Zhang et al. (2014)
0.352	$83.0 \pm 14.0$	Moresco et al. (2012)
0.3802	$83.0 \pm 13.5$	Moresco et al. (2016)
0.4	$95.0 \pm 17.0$	Simon et al. (2005)
0.4004	$77.0 \pm 10.2$	Moresco et al. (2016)
0.4247	$87.1 \pm 11.2$	Moresco et al. (2016)
0.4497	$92.8 \pm 12.9$	Moresco et al. (2016)
0.47	$89.0 \pm 50.0$	Ratsimbazafy et al. (2017)
0.4783	$80.9 \pm 9.0$	Moresco et al. (2016)
0.48	$97.0 \pm 62.0$	Stern et al. (2010)
0.593	$104.0 \pm 13.0$	Moresco et al. (2012)
0.68	$92.0 \pm 8.0$	Moresco et al. (2012)
<b>0.75</b>	<b><math>98.8 \pm 33.6</math></b>	<b>Borghi et al. (2022)</b>
0.781	$105.0 \pm 12.0$	Moresco et al. (2012)
0.875	$125.0 \pm 17.0$	Moresco et al. (2012)
0.88	$90.0 \pm 40.0$	Stern et al. (2010)
0.9	$117.0 \pm 23.0$	Simon et al. (2005)
1.037	$154.0 \pm 20.0$	Moresco et al. (2012)
1.3	$168.0 \pm 17.0$	Simon et al. (2005)
1.363	$160.0 \pm 33.6$	Moresco (2015)
1.43	$177.0 \pm 18.0$	Simon et al. (2005)
1.53	$140.0 \pm 14.0$	Simon et al. (2005)
1.75	$202.0 \pm 40.0$	Simon et al. (2005)
1.965	$186.5 \pm 50.4$	Moresco (2015)

<sup>a</sup> km sec<sup>-1</sup> Mpc<sup>-1</sup>.

On the other hand, if we have a power-law like relation between three components i.e.  $a = (bc)^n$ , then to reconstruct a linear relation for such power-law relation, we take logarithms on both sides and thus can re-plot a ternary diagram between  $\log_{10}(a)$ ,  $-n \log_{10}(b)$  and  $-n \log_{10}(c)$  and every point on this ternary plot satisfy the condition  $\log_{10}(a) - n \log_{10}(b) - n \log_{10}(c) = 0$ . Thus, by knowing any two out of the three parameters, one can put constraints on the third parameter. In this work, we focus on a power-law relation between cosmological parameters and put constraints on these parameters. We show that such a representation represents the cosmic constraints in an intuitive and illustrative manner.

### 3.2 Hubble Phase Space Portrait (HPSP)

For a spatially flat, homogeneous and isotropic universe, the Friedmann equations are

$$\left(\frac{\dot{a}}{a}\right)^2 = \frac{8\pi G}{3} \rho_T \quad (2)$$

$$2\frac{\ddot{a}}{a} + \left(\frac{\dot{a}}{a}\right)^2 = -8\pi G p_T \quad (3)$$

In these equations,  $a(t)$  is scale factor,  $\rho_T$  and  $p_T$  denote the total energy density and total pressure respectively. By considering  $H(t) = \frac{\dot{a}}{a}$  and so  $\dot{H} + H^2 = \frac{\ddot{a}}{a}$  and dividing equation (3) by equation (2), we get

$$\dot{H} = -\frac{3}{2}(1 + \omega)H^2 \quad (4)$$

where we consider an equation of state parameter  $\omega$  which

relates the total energy density to total pressure of a barotropic fluid via  $p_T = \omega \rho_T$ . Depending on the content of the universe,  $\omega$  takes values in the range  $-1 \leq \omega \leq \frac{1}{3}$ . Thus we can reconstruct Friedmann's equations into a single equation i.e.  $\dot{H} = F(H)$ . Using this equation, by visualizing the trajectories in the  $(H, \dot{H})$  phase space, one can analyze different cosmic models in a clear and transparent way. Equation (4) is referred to as the phase portrait and its solution is the phase trajectory. For more details about phase-space portrait, please refer El Hanafy & Nashed (2017); Awad et al. (2018); El-Zant et al. (2019). Corresponding to any theory, the phase portrait can be drawn in  $(H, \dot{H})$  phase-space. For example, a theoretical reconstruction of the Hubble phase space portrait for different cosmological models is shown in Figure 1.

In this framework, we classify the different phases of Figure 1 as follows:

(i) In  $(H, \dot{H})$  phase space, the left half represent a contracting universe since this portion has  $H < 0$ . On the other hand, the right half has  $H > 0$ , which represents an expanding universe.

(ii) For different values of the equation of state parameter,  $\omega$ , we can draw lines in the  $(H, \dot{H})$  phase space. For example, for a matter dominated universe we draw the phase trajectory corresponding to  $\omega = 0$ . Similarly, we plot lines for radiation dominated, curvature dominated and cosmological constant dominated universes corresponding to  $\omega = 1/3$ ,  $\omega = -1/3$  and  $\omega = -1$  respectively.

(iii) The line corresponding to  $w = -1/3$  is generally referred as "zero acceleration curve" since the deceleration parameter for this line is zero i.e.  $q = 0$ . This line splits the  $(H, \dot{H})$  phase space into two regions. The upper region represents the accelerated universe where we have  $\omega < -1/3$  and  $q < 0$ . On the other hand, the lower region shows the decelerated universe. In this region, the equation of state parameter is  $\omega > -1/3$  and deceleration parameter is  $q > 0$ .

(iv) Therefore, the full  $(H, \dot{H})$  phase space is divided into four different regions. The upper left region represents an **accelerated contraction** of universe since  $H < 0$  and  $q < 0$ . The upper right displays an **accelerated expansion** of universe since  $H > 0$  and  $q < 0$ . The lower left represents a **decelerated contraction** of universe where  $H < 0$  and  $q > 0$ . And the lower right region represents a **decelerated expansion** of universe since in this region, we have  $H > 0$  and  $q > 0$ .

As we know, the universe has passed from radiation dominated ( $\omega = 1/3$ ) to matter dominated ( $\omega = 0$ ) eras in the past. The lower regions characterized the usual FLRW models. As a result we expect that the observations will lie in that region which will show a transition from a decelerated expansion era to an accelerated expansion era by crossing the zero-acceleration ( $q = 0$ ) line. The value of the Hubble parameter corresponding to this crossing point is referred to as the transition Hubble parameter value and the corresponding redshift is called the transition redshift. By analyzing the  $(H, \dot{H})$  phase space, one can easily estimate the transition Hubble parameter value and transition redshift value. Hence, in this analysis, we focus only on this inner right region of the  $(H, \dot{H})$  phase space.

### 3.3 Statistical Methods

In this work, we use the recent compilation of Hubble parameter measurements. This dataset has measurements of redshift  $z$ , Hubble parameter  $H(z)$  and uncertainties in the Hubble parameter  $\sigma_H(z)$ . For the first part (the cosmic triangle) of this work, we assume a non-flat  $\Lambda$ CDM model as a background cosmological model and by

minimizing the Chi-square, we put constraints on the cosmological parameters. Further, in second part, we apply Gaussian Process to reconstruct the Hubble parameter and its derivative from Hubble parameter measurements as explained below.

#### 3.3.1 Chi-square Analysis

The cosmological parameters of the assumed background cosmological model are determined by maximizing the likelihood  $\mathcal{L} \sim \exp(-\chi^2/2)$ , where Chi-square  $\chi^2$  is

$$\chi^2(\mathbf{P}) = \sum_{i=1}^{n=32} \frac{(H_{th}(z_i; \mathbf{P}) - H_{obs}(z_i))^2}{\sigma_T^2(z_i)} \quad (5)$$

Here,  $\mathbf{P}$  represents the cosmological parameters i.e.  $H_0, \Omega_{m0}, \Omega_{k0}$  and  $\Omega_{\Lambda 0}$ , where as  $H_{th}$  and  $H_{obs}$  are the theoretical Hubble parameter and observed Hubble parameter respectively. To remove the dependency of  $H_0$  on the other cosmological parameters, and by considering a flat prior for  $H_0$ , we marginalize the Chi-square over  $H_0$  and thus equation (5) becomes

$$\tilde{\chi}^2 = \mathbf{A} - \frac{\mathbf{B}^2}{\mathbf{C}} + \ln \frac{\mathbf{C}}{2\pi} \quad (6)$$

$$\text{Here, } \mathbf{A} = \sum_{i=1}^{32} \frac{H_{obs}^2}{\sigma_T^2(z_i)}, \mathbf{B} = \sum_{i=1}^{32} \frac{H_{obs} E(z_i; \mathbf{P})}{\sigma_T^2(z_i)} \quad \&$$

$$\mathbf{C} = \sum_{i=1}^{32} \frac{E^2(z_i; \mathbf{p})}{\sigma_T^2(z_i)}$$

where,

$$E(z; \Omega_{m0}, \Omega_{k0}) = \sqrt{\Omega_{m0}(1+z)^3 + \Omega_{k0}(1+z)^2 + 1 - \Omega_{m0} - \Omega_{k0}}$$

Here  $\sigma_T^2$  is the total uncertainty in the Hubble parameter which includes the effect of both statistical errors as well as systematic errors. Thus in our analysis, we consider full covariance matrix  $\text{Cov}_{ij}$  as

$$\text{Cov}_{ij} = \text{Cov}_{ij}^{\text{stat}} + \text{Cov}_{ij}^{\text{sys}}, \quad (7)$$

where  $\text{Cov}_{ij}^{\text{stat}}$  denote the contributions to the covariance due to statistical errors. The contribution due to systematic errors is given by  $\text{Cov}_{ij}^{\text{sys}}$ . To compute the systematic errors carefully we refer to the analysis carried by Moresco et al. (2020) where, we have considered the main four contributions in the covariance matrix i.e. initial mass function, stellar library, metallicity, and stellar population synthesis models. For a detailed discussion of the full covariance matrix please refer to Section-3.1.4 of Moresco et al. (2022).

#### 3.3.2 Gaussian Process

The aim of the Gaussian Process (GP) method is to reconstruct a function from data without assuming a parametrized form of the function. For example, we have values  $H(z)$  from a set of measurements i.e.  $H(z_i) \pm \sigma_H$ , where the value of  $H(z_i)$  follows a Gaussian distribution at every point of  $z_i$ . Suppose we want the value of the function at an unknown point  $z'$ . For this a covariance or kernel function  $k(z, z')$  is needed which indicates that the value of the function at  $z$  is not independent of its value at  $z'$  but is correlated by  $k(z, z')$ .

Thus, the Gaussian Process technique is non-parametric since it is dependent on the choice of the covariance function rather than

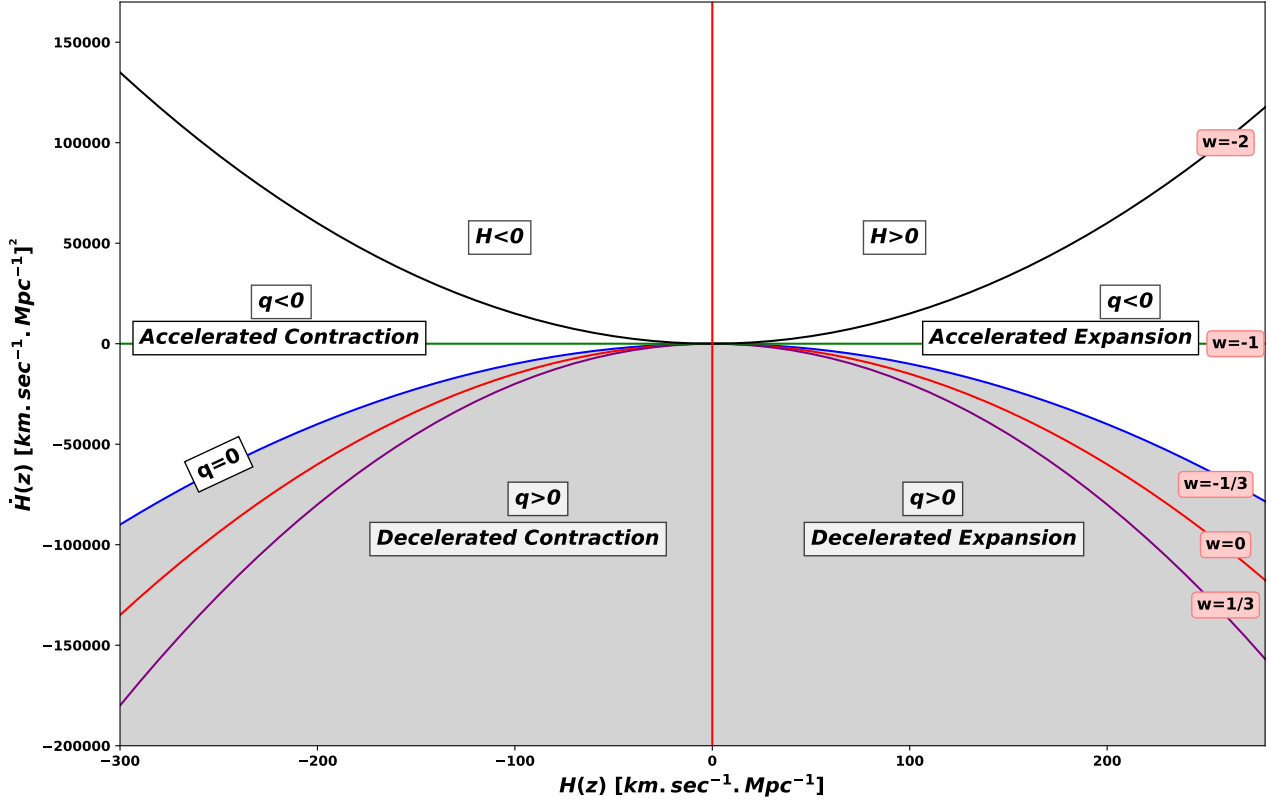


Figure 1. The theoretical reconstruction of Hubble phase space portrait.

a set of parameters in an assumed model or functional form. In general, the covariance function depends only on the distance between the points  $|z - z'|$ . Here, we consider the Squared Exponential (or Gaussian) kernel function (Moresco et al. (2012); Ó Colgáin & Sheikh-Jabbari (2021)) since this function has the characteristic of being infinitely differentiable, which is important for reconstructing a function's derivative. The Squared Exponential kernel function is

$$k(z, z') = \sigma_f^2 \exp\left(-\frac{(z - z')^2}{2\ell^2}\right) \quad (8)$$

where,  $\sigma_f$  and  $\ell$  are referred as the GP hyperparameters. These basically regulate the correlation-strength of the function value and the length scale of the correlation in  $z$  respectively. By minimizing a log marginal likelihood function, one can calculate the value of  $\sigma_f$  and  $\ell$  using the observed data. For maximization, we use flat priors for  $\sigma_f$  and  $\ell$  for a particular choice of kernel function.

This method can also be used to reconstruct the derivative of the function i.e.  $H'(z)$ . While reconstructing the derivative of a function the covariance between the observational points remains unchanged. However, we also need a covariance between the function and its derivative as well as the covariance between the derivatives.

Finally, the Gaussian Process for  $H(z)$  and for its derivative  $H'(z)$  are

$$\begin{aligned} H(z) &\sim \mathcal{GP}(\mu(z), k(z, z')) \\ H'(z) &\sim \mathcal{GP}\left(\mu'(z), \frac{\partial^2 k(z, z')}{\partial z \partial z'}\right) \end{aligned} \quad (9)$$

where  $\mu(z)$  is the mean value of a given function i.e  $H(z)$  In this

analysis, we use equation (9) to reconstruct the Hubble parameter  $H(z)$  as well as the derivative of the Hubble parameter  $H'(z)$  using 32 datapoints of Hubble parameter measurements.

### 3.3.3 Generation of simulated $H(z)$ data

It seems natural that future observations will enlarge the present dataset of Hubble parameter. To study the impact of a potentially enlarged dataset, we use a mock dataset of the Hubble parameter measurements and study its impact on the cosmic triangle and Hubble phase space portrait. To simulate the Hubble parameter data, we use the simulation method as explained by Ma & Zhang (2011). The simulation steps are as follows:

(i) We choose the flat  $\Lambda$ CDM model as a fiducial cosmological model and adopt the best fit values of  $H_0, \Omega_{m0}$  from Planck Collaboration et al. (2020). Using these values, we calculate the fiducial value of Hubble parameter i.e.  $H_{fid}(z)$ .

(ii) To update the errors of observed Hubble parameter measurements, we plot their errorbars versus redshift and based on the fact that the errors of  $H(z)$  seem to increase almost linearly, with respect to  $z$ , we identify 7 datapoints as outliers and exclude them.

(iii) By using the remaining Hubble parameters points, to estimate the errors of the simulated data, we draw upper and lower lines which are  $\sigma^+(z) = 16.577z + 18.440$  and  $\sigma^-(z) = 7.402z + 2.675$  respectively. To predict the mean error for future observations, the midline of the errors is  $\sigma^0(z) = 11.990z + 10.558$ .

(iv) By assuming a Gaussian distribution of the simulated datapoints, the error of the simulated  $H(z)$  is a random number drawn from a Gaussian distribution with mean  $\sigma^0(z)$  and variance  $\epsilon(z)$  i.e.  $\tilde{\sigma}(z) = \mathcal{N}[\sigma^0(z), \epsilon(z)]$ , where we define the

**Table 2.** The best fit values of  $\Omega_{m0}$ ,  $\Omega_{k0}$  and  $\Omega_{\Lambda0}$  with  $1\sigma$  confidence level obtained by using 32  $H(z)$  measurements.

Parameter	Best fit value [ $1\sigma$ C.L.]
$\Omega_{m0}$	$0.380^{+0.318}_{-0.375}$
$\Omega_{k0}$	$-0.186^{+1.137}_{-0.864}$
$\Omega_{\Lambda0}$	$0.806^{+0.544}_{-0.806}$

$\epsilon(z) = \frac{\sigma^+(z) - \sigma^-(z)}{4}$ . The parameter  $\epsilon(z)$  is set so that there is a 95.4% chance of probability of  $\tilde{\sigma}(z)$  within the strip.

(v) The value of simulated Hubble parameter are defined as  $H_{sim} = H_{fid} + \Delta H$ , where  $\Delta H$  can be derived from a Gaussian distribution of the form  $\mathcal{N}[0, \tilde{\sigma}(z)]$ .

Using the above steps, we have generated 100 simulated values of the Hubble parameter as well as the uncertainties in the Hubble parameter.

## 4 RESULTS

In this paper, our aim is to put constraints on the transition redshift  $z_t$  from Hubble parameter measurements using both model-dependent and model-independent approaches. In the first part, we propose a cosmic triangle plot to put constraints on the transition redshift. For this purpose, we consider a non-flat  $\Lambda$ CDM model as a background cosmology and put constraints on its cosmological parameters. In the second part, we reconstruct the Hubble Phase Space Portrait using Gaussian Process and put constraints on the transition redshift as well as on the equation of state parameter in a model-independent way.

### 4.1 The Cosmic Triangle

In this part, we consider the non-flat  $\Lambda$ CDM model

$$H(z) = H_0 \sqrt{\Omega_{m0}(1+z)^3 + \Omega_{k0}(1+z)^2 + \Omega_{\Lambda0}} \quad (10)$$

where,  $\Omega_{\Lambda0} = 1 - \Omega_{m0} - \Omega_{k0}$  and  $H_0$  is the Hubble constant. In this model, we are left with three free parameters i.e.  $H_0$ ,  $\Omega_{m0}$  and  $\Omega_{k0}$ . To reduce the number of free parameters, we marginalise over  $H_0$  and using Hubble parameter measurements we put constraints on  $\Omega_{m0}$  and  $\Omega_{k0}$  by minimising the Chi-square. The best fit values of the parameters are given in Table 2.

The best fit value of  $\Omega_{k0} = -0.186^{+1.137}_{-0.864}$  as shown in Table 2 suggests a spatially flat universe at  $1\sigma$  confidence level which is in good agreement with [Planck Collaboration et al. \(2020\)](#). The 2D contour plot of  $\Omega_{m0}$  versus  $\Omega_{k0}$  is shown in Figure 2.

Using the parameters  $\Omega_{m0}$ ,  $\Omega_{k0}$  and  $\Omega_{\Lambda0}$ , we have drawn a triangle plot as shown in Figure 3. The intersection in the ternary plot shows the best fit value of each parameter and the contour like shape indicates the joint  $1\sigma$  confidence level.

Further, for the transition epoch, we equate the deceleration parameter  $q(z)$  to zero at redshift  $z_t$ . Then using the Friedmann equation, the value of the transition redshift in terms of cosmological parameters is given by

$$z_t = \left( \frac{2\Omega_{\Lambda0}}{\Omega_{m0}} \right)^{1/3} - 1, \quad \text{where, } \Omega_{m0} + \Omega_{k0} + \Omega_{\Lambda0} = 1 \quad (11)$$

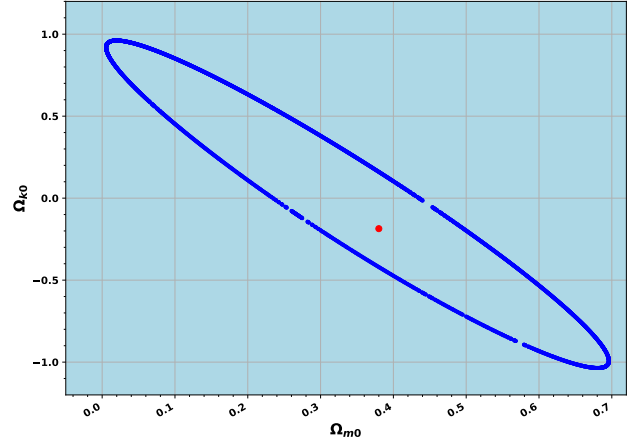


**Figure 2.** 2D contour plot of  $\Omega_{m0}$  versus  $\Omega_{k0}$  with their  $1\sigma$  confidence level, where the red dot denotes the best fit value of the parameters.

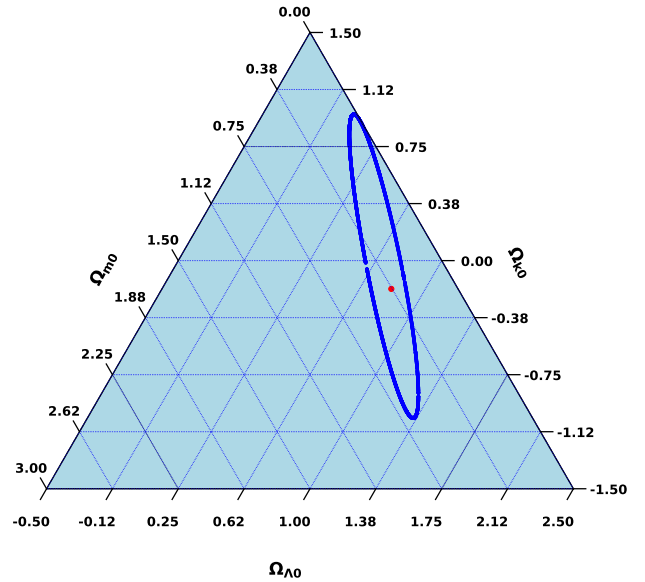


**Figure 3.** The cosmic triangle plot among  $\Omega_{m0}$ ,  $\Omega_{k0}$  and  $\Omega_{\Lambda0}$  with their  $1\sigma$  confidence level, where the red dot denotes the best fit value of the parameters.

Thus using the constraints of  $\Omega_{m0}$ ,  $\Omega_{k0}$  and  $\Omega_{\Lambda0}$ , the best fit value of transition redshift comes out to be  $z_t = 0.619^{+0.580}_{-0.758}$ . To plot a triangle plot we require a linear relation among its three components. By keeping this in mind, we take the logarithm of equation (11) as shown in equation (12)

$$\log_{10}(\Omega_{m0}) - \log_{10}(2\Omega_{\Lambda0}) + 3 \log_{10}(1+z_t) = 0 \quad (12)$$

Using this linear relation, we reconstruct a triangle plot among  $\log_{10}(\Omega_{m0})$ ,  $\log_{10}(2\Omega_{\Lambda0})$  and  $3 \log_{10}(1+z_t)$  as shown in Figure 4.

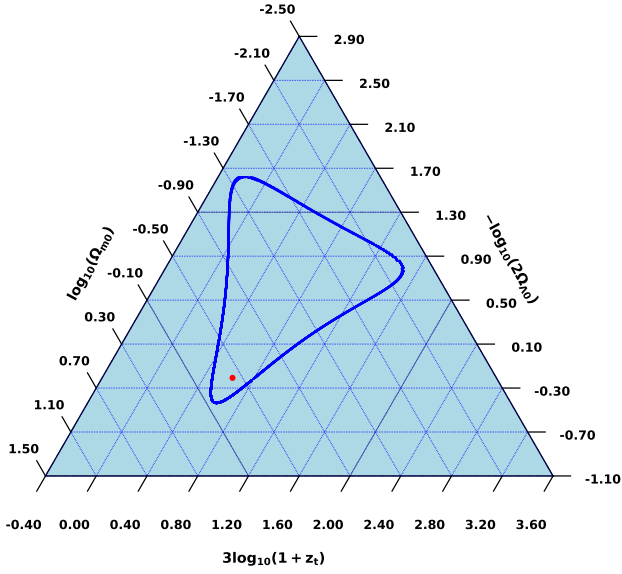


**Figure 4.** The cosmic triangle plot among  $\log_{10}(\Omega_{m0})$ ,  $-\log_{10}(2\Omega_{\Lambda 0})$  and  $3\log_{10}(1+z_t)$ , with their  $1\sigma$  confidence level.

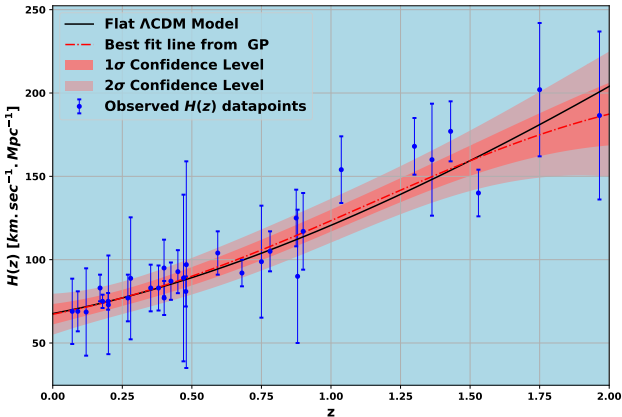


**Figure 5.** Hubble Parameter reconstruction using Gaussian Process.

## 4.2 Hubble Phase Space Portrait (HPSP)

The equation for the phase portrait is

$$\dot{H}(z) = -\frac{3}{2}(1+\omega)H^2(z) \quad (13)$$

To plot this phase space portrait for  $H$ , we need to calculate the Hubble parameter  $H(z)$  and its derivative  $H'(z)$ . For this, we use **GaPP**, a Python based Gaussian Process tool developed by [Seikel et al. \(2012\)](#) which provides the reconstruction of  $H(z)$  as shown in Figure 5.

The Gaussian Process, as operated by GaPP, reconstructs not only  $H(z)$  from data, but it also helps us to reconstruct its derivative and the associated uncertainties. For the phase portrait, we need to estimate the time-derivative of the Hubble parameter i.e.  $\dot{H}(z)$ . The relation between  $H'(z)$  and  $\dot{H}(z)$  is

$$\dot{H}(z) = -(1+z)H(z)H'(z) \quad (14)$$

Thus, by using the reconstructed  $H'(z)$ , we can estimate  $\dot{H}(z)$

as well as its uncertainties. Using  $H(z)$  and  $H'(z)$ , we have drawn the Hubble Phase Space Portrait (HPSP) between  $\dot{H}(z)$  versus  $H(z)$  as shown in Figure 6.

In this diagram, as expected the best fit line (in red colour) is reconstructed using Gaussian process which evolve from decelerated expansion region to accelerated expansion region. The point where the best fit line crosses the zero-acceleration curve is generally referred to as the transition point and the redshift corresponding to it turns out to be  $z_t = 0.591 \pm 0.365$ , which is in good agreement with the recent results of [Planck Collaboration et al. \(2020\)](#). Further, using equation (13) and by following the reconstructed  $H(z)$  and  $\dot{H}(z)$ , we obtain the present value of equation of state is  $\omega_0 = -0.677 \pm 0.284$ .

## 4.3 Results from the simulated data sets

So far, we have discussed the results of the cosmic triangle diagram and Hubble Phase Space Portrait using 32 datapoints of Hubble parameter measurements. Due to the limited number of datapoints, we find large uncertainties and hence a wider region in both cosmic triangle and HPSP diagrams. In order to estimate the impact of future enhancement of the data, we use mock data set of the Hubble parameter measurements and study the potential of using this type of data for the cosmic triangle and Hubble phase space portrait. To simulate the Hubble parameter data we use the simulation method as described by [Ma & Zhang \(2011\)](#). As explained in Section 3 we have generated 100 simulated values of the Hubble parameter. The simulated datapoints are shown in Figure 7 along with the observed Hubble parameter measurements.

We re-plot the cosmic triangle diagram as shown in Figure 8 by using 100 simulated datapoints of Hubble parameter. We find the transition redshift as  $z_t = 0.588^{+0.386}_{-0.391}$  and as expected the contours have shrunk substantially.

Further, using the same simulated Hubble parameter dataset, we update the Hubble phase space diagram as shown in Figure 9. The best fit value of the transition redshift in this case comes out to be  $z_t = 0.594 \pm 0.279$  which is consistent with the [Planck Collaboration et al. \(2020\)](#) at  $1\sigma$  confidence level. In this case, the present value of equation of state is  $\omega_0 = -0.623 \pm 0.249$ .

The summary of different value of transition redshift obtained from different surveys are shown in Table 3.

## 5 DISCUSSION AND CONCLUSIONS

That the universe is in a phase of accelerated expansion is now well established. Given this, it is an interesting exercise to determine the epoch of the transition from a decelerated phase to the accelerated phase. In this work, we use the recent dataset for Hubble parameter and full covariance matrix for systematic uncertainties to put constraints on the transition redshift both in a model-dependent and model independent way. The main conclusions are as follows:

### Part-A: The Cosmic Triangle

We consider a non-flat  $\Lambda$ CDM model as a background cosmological model. By marginalizing over  $H_0$  and minimizing the Chi-square, we put constraints on cosmological parameters i.e.  $z_t$ ,  $\Omega_{m0}$ , and  $\Omega_{\Lambda 0}$ . Further, using  $z_t$ ,  $\Omega_{m0}$ , and  $\Omega_{\Lambda 0}$ , we reconstruct the cosmic triangle which allows us to visualize the confidence region in an intuitive and illustrative way. The main conclusions of this part are as follows:

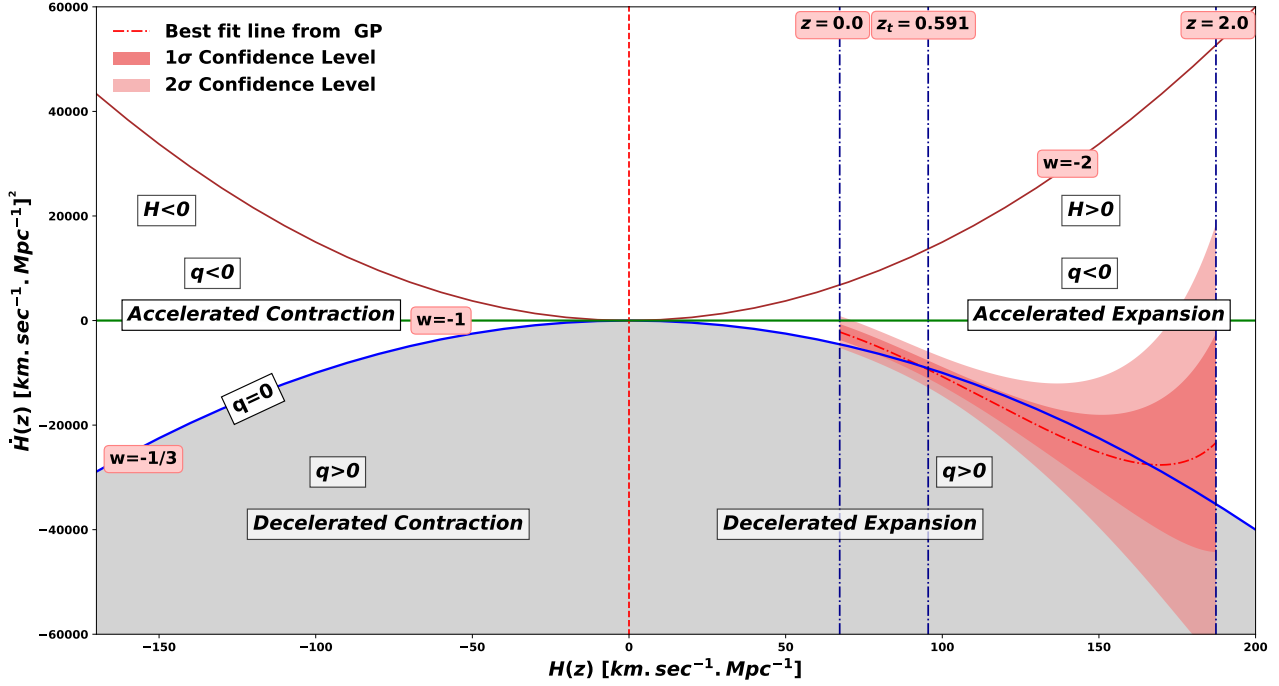


**Figure 6.** The Hubble Phase Space Portrait obtained by applying Gaussian process on observed  $H(z)$  datapoints.

**Table 3.** Constraints on  $z_t$  from different cosmological observations.

Dataset	Methodology	Best fit value of $z_t$	Reference
BAO, CMB, SNe	Kinematic: $\omega(z)$	$\sim 0.7$	<a href="#">Magaña et al. (2014)</a>
Age of Galaxies, Strong Lensing, SNe	Kinematic: $q(z)$	$< 1$	<a href="#">Rani et al. (2015)</a>
H(z): CC	$\Lambda$ CDM Model	$0.64^{+0.11}_{-0.07}$	<a href="#">Moresco et al. (2016)</a>
H(z): CC+BAO	$\Lambda$ CDM Model	$0.72^{+0.05}_{-0.05}$	<a href="#">Farooq et al. (2017)</a>
H(z): CC+BAO, SNe	Kinematic Quadratic $H(z)$	$0.870^{+0.063}_{-0.063}$	<a href="#">Jesus et al. (2018)</a>
Planck-2018	$\Lambda$ CDM Model	$0.632^{+0.018}_{-0.018}$	<a href="#">Planck Collaboration et al. (2020)</a>
SNe: Pantheon	Gaussian Process	$0.683^{+0.110}_{-0.082}$	<a href="#">Lin et al. (2019)</a>
H(z): CC+BAO	Gaussian Process	$0.59^{+0.12}_{-0.11}$	<a href="#">Jesus et al. (2020)</a>
H(z): CC+BAO, SNe	$\Lambda$ CDM Model	$0.69^{+0.25}_{-0.25}$	<a href="#">Velasquez-Toribio &amp; Magnago (2020)</a>
H(z): CC+BAO	Gaussian Process	$0.637^{+0.165}_{-0.175}$	<a href="#">Velasquez-Toribio &amp; Fabris (2022)</a>
Updated H(z): CC	Observed Cosmic Triangle	$0.619^{+0.580}_{-0.758}$	This work
Simulated H(z): CC	Simulated Cosmic Triangle	$0.588^{+0.386}_{-0.391}$	This work
Updated H(z): CC	Observed HPSP	$0.591^{+0.365}_{-0.365}$	This work
Simulated H(z): CC	Simulated HPSP	$0.594^{+0.279}_{-0.279}$	This work

(i) The best fit value of the cosmic curvature parameter ( $\Omega_{k0}$ ) suggests an closed universe but a spatially flat universe can be accommodated at  $1\sigma$  confidence level. Thus our results are compatible with [Planck Collaboration et al. \(2020\)](#) at  $1\sigma$  confidence level.

(ii) We find that the 2D contour between  $\Omega_{m0}$  and  $\Omega_{k0}$  shows a strong negative correlation between them.

(iii) The cosmic triangle representation among  $\Omega_{m0}$ ,  $\Omega_{k0}$  and  $\Omega_{\Lambda0}$  shows a joint confidence level in 2D space instead of 3D. We find that this representation allows us to visualize these three parameters simultaneously in a single 2D plot.

(iv) Using an updated cosmic triangle plot among  $\log_{10}(\Omega_{m0})$ ,  $-\log_{10}(2\Omega_{\Lambda0})$  and  $3\log_{10}(1+z_t)$  we put constraints on the transition redshift, which is in agreement with the result obtained from the different observables as listed in Table 3.

(v) We generate a mock dataset of 100 datapoints by adopting a fiducial flat  $\Lambda$ CDM model. Using this simulated dataset, we find that the results are consistent with the [Planck Collaboration et al. \(2020\)](#). Further, as expected, the confidence region between these parameters becomes substantially tight.

### Part-B: Hubble Phase Space Portrait (HPSP)

In this part, we consider the observed value of the Hubble parameter to draw a phase space ( $H, \dot{H}$ ) portrait. Our main conclusions are listed below-

(i) We emphasize that the analysis with HPSP provides a way to estimate the transition redshift as well as the current value of the



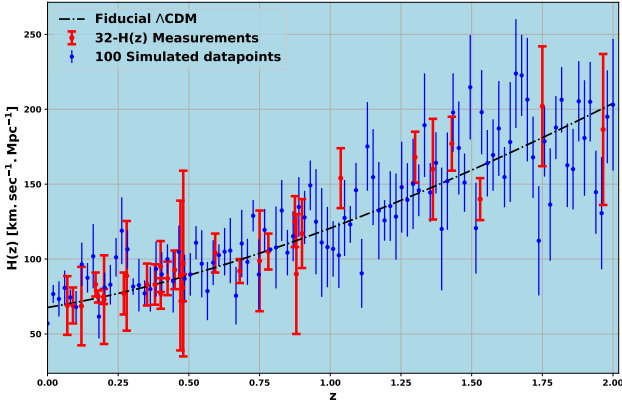


**Figure 7.** The simulated datapoints of  $H(z)$  in the redshift  $0.0 < z < 2.0$ . The blue points represent the simulated datapoints and the observed  $H(z)$  are represented by the red colour.

equation of state parameter without solving any equations for these cosmological parameters.

(ii) In the HPSP, the reconstructed best fit line lies in the matter-dominated era at higher redshift, which indicates that the universe was in decelerated phase. Further, as expected, the best fit line crosses the transition boundary from deceleration to acceleration at a redshift,  $z_t$ . This characteristic of HPSP is in agreement with the standard model of cosmology. The reconstructed best fit line in HPSP is in agreement with the thermal history of universe and can be used to estimate the transition redshift. The result obtained using HPSP also is in agreement with the results obtained from different observables as listed in Table 3.

(iii) From HPSP, the constraint obtained on the present value of the equation of state parameter ( $\omega_0$ ) shows agreement with the Planck Collaboration et al. (2020).

(iv) Using the mock datapoints of Hubble parameter measurements, we reconstruct the HPSP and estimate the transition redshift value. This result is highly consistent with the results obtained in the previous part (The Cosmic Triangle).

## ACKNOWLEDGEMENTS

Authors would like to thank Michele Moresco and Eoin Ó Colgáin for their constructive and useful suggestions that helped to improve the work. Darshan thanks Jose Luis Bernal for valuable discussion. Darshan is supported by an INSPIRE Fellowship under the reference number: IF180293 [SRF], DST India. Darshan acknowledges facilities provided by the IUCAA Centre for Astronomy Research and Development (ICARD), University of Delhi. This research work made use of the free Python packages NUMPY Harris et al. (2020), MATPLOTLIB Hunter (2007), GAPP (Seikel et al. (2012)), and PYTHON-TERNARY (Harper et al. (2015)).

## DATA AVAILABILITY

The data generated as part of this project may be shared on a reasonable request to the corresponding author.

## REFERENCES

Amanullah R., et al., 2010, *ApJ*, 716, 712

- Astier P., et al., 2006, *A&A*, 447, 31
- Awad A., El Hanafy W., Nashed G. G. L., Saridakis E. N., 2018, *J. Cosmology Astropart. Phys.*, 02, 052
- Bahcall N. A., Ostriker J. P., Perlmutter S., Steinhardt P. J., 1999, *Science*, 284, 1481
- Bassett B., Hlozek R., 2010, in Ruiz-Lapuente P., ed., , Dark Energy: Observational and Theoretical Approaches. p. 246
- Benítez N., et al., 2009, *ApJ*, 691, 241
- Bernal J. L., Verde L., Jimenez R., Kamionkowski M., Valcin D., Wandelt B. D., 2021, *Phys. Rev. D*, 103, 103533
- Borghini N., Moresco M., Cimatti A., 2022, *ApJ*, 928, L4
- Cai R.-G., Tuo Z.-L., 2011, *Physics Letters B*, 706, 116
- Capozziello S., Luongo O., Saridakis E. N., 2015, *Phys. Rev. D*, 91, 124037
- Cuceu A., Farr J., Lemos P., Font-Ribera A., 2019, *J. Cosmology Astropart. Phys.*, 10, 044
- Cunha J. V., Lima J. A. S., 2008, *MNRAS*, 390, 210
- Davis T. M., et al., 2007, *ApJ*, 666, 716
- Dawson K. S., et al., 2013, *AJ*, 145, 10
- Eisenstein D. J., et al., 2005, *ApJ*, 633, 560
- Eisenstein D. J., et al., 2011, *AJ*, 142, 72
- El Hanafy W., Nashed G. G. L., 2017, *Chinese Physics C*, 41, 125103
- El-Zant A., El Hanafy W., Elgammal S., 2019, *ApJ*, 871, 210
- Elgarøy Ø., Multamäki T., 2006, *J. Cosmology Astropart. Phys.*, 09, 002
- Farooq O., Ratra B., 2013, *ApJ*, 766, L7
- Farooq O., Crandall S., Ratra B., 2013a, *Physics Letters B*, 726, 72
- Farooq O., Mania D., Ratra B., 2013b, *ApJ*, 764, 138
- Farooq O., Ranjeet Madiyar F., Crandall S., Ratra B., 2017, *ApJ*, 835, 26
- Gaztañaga E., Cabré A., Hui L., 2009, *MNRAS*, 399, 1663
- Gong Y., Wang A., 2007, *Phys. Rev. D*, 75, 043520
- Goobar A., Dhawan S., Scolnic D., 2018, *MNRAS*, 477, L75
- Harper M., et al., 2015, *Zenodo*, 12, 17
- Harris C. R., et al., 2020, *Nature*, 585, 357
- Hunter J. D., 2007, *Computing in Science and Engineering*, 9, 90
- Huterer D., Shafer D. L., 2018, *Reports on Progress in Physics*, 81, 016901
- Jesus J. F., Holanda R. F. L., Pereira S. H., 2018, *J. Cosmology Astropart. Phys.*, 05, 073
- Jesus J. F., Valentim R., Escobal A. A., Pereira S. H., 2020, *J. Cosmology Astropart. Phys.*, 04, 053
- Jimenez R., Verde L., Treu T., Stern D., 2003, *ApJ*, 593, 622
- Komatsu E., et al., 2011, *ApJS*, 192, 18
- Kowalski M., et al., 2008, *ApJ*, 686, 749
- Larson D., et al., 2011, *ApJS*, 192, 16
- Lima J. A. S., Holanda R. F. L., Cunha J. V., 2009, arXiv e-prints, p. arXiv:0905.2628
- Lima J. A. S., Jesus J. F., Santos R. C., Gill M. S. S., 2012, arXiv e-prints, p. arXiv:1205.4688
- Lin H.-N., Li X., Tang L., 2019, *Chinese Physics C*, 43, 075101
- Ma C., Zhang T.-J., 2011, *ApJ*, 730, 74
- Magaña J., Cárdenas V. H., Motta V., 2014, *J. Cosmology Astropart. Phys.*, 10, 017
- Magaña J., Amante M. H., Garcia-Aspeitia M. A., Motta V., 2018, *MNRAS*, 476, 1036
- Martin J., 2012, *Comptes Rendus Physique*, 13, 566
- McVittie G. C., 1962, *ApJ*, 136, 334
- Melchiorri A., Pagano L., Pandolfi S., 2007, *Phys. Rev. D*, 76, 041301
- Moresco M., 2015, *MNRAS*, 450, L16
- Moresco M., et al., 2012, *J. Cosmology Astropart. Phys.*, 08, 006
- Moresco M., et al., 2016, *J. Cosmology Astropart. Phys.*, 05, 014
- Moresco M., Jimenez R., Verde L., Cimatti A., Pozzetti L., 2020, *ApJ*, 898, 82
- Moresco M., et al., 2022, arXiv e-prints, p. arXiv:2201.07241
- Nair R., Jhingan S., Jain D., 2012, *J. Cosmology Astropart. Phys.*, 01, 018
- Ó Colgáin E., Sheikh-Jabbari M. M., 2021, *European Physical Journal C*, 81, 892
- Percival W. J., Cole S., Eisenstein D. J., Nichol R. C., Peacock J. A., Pope A. C., Szalay A. S., 2007, *MNRAS*, 381, 1053
- Perlmutter S., et al., 1999, *ApJ*, 517, 565
- Planck Collaboration et al., 2020, *A&A*, 641, A6

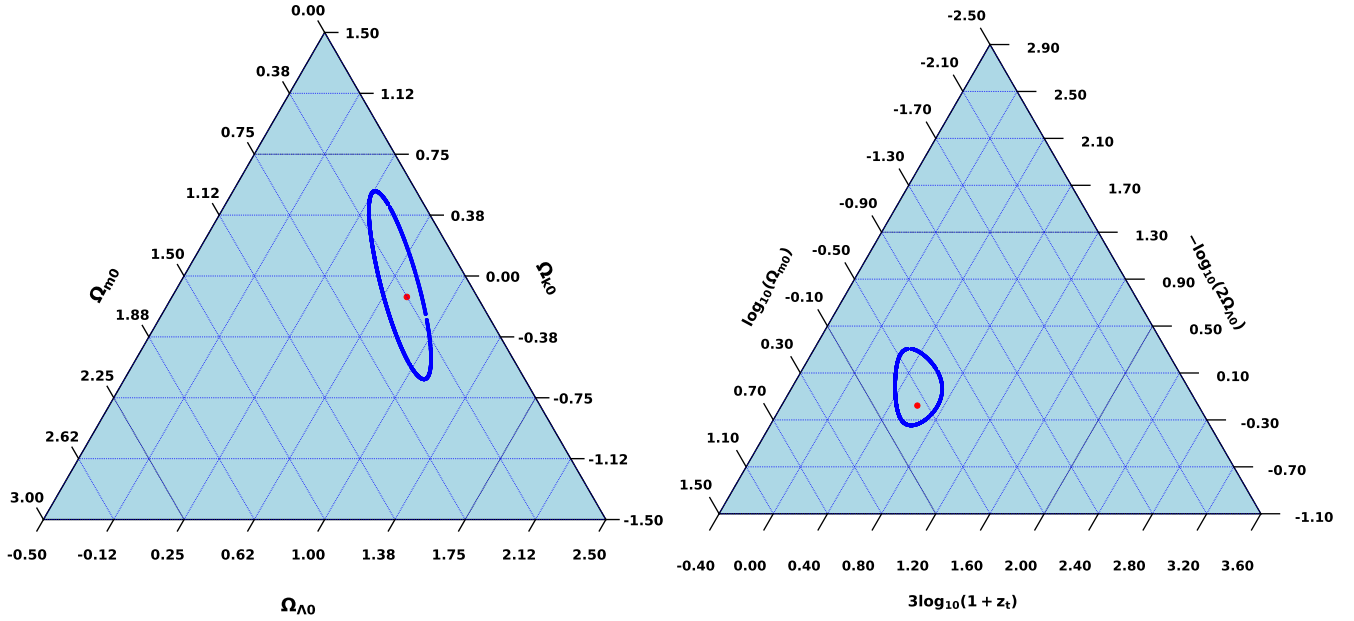


Figure 8. The cosmic triangle diagrams using 100 simulated Hubble parameter datapoints, where the red dot denotes the best fit value of the parameters.

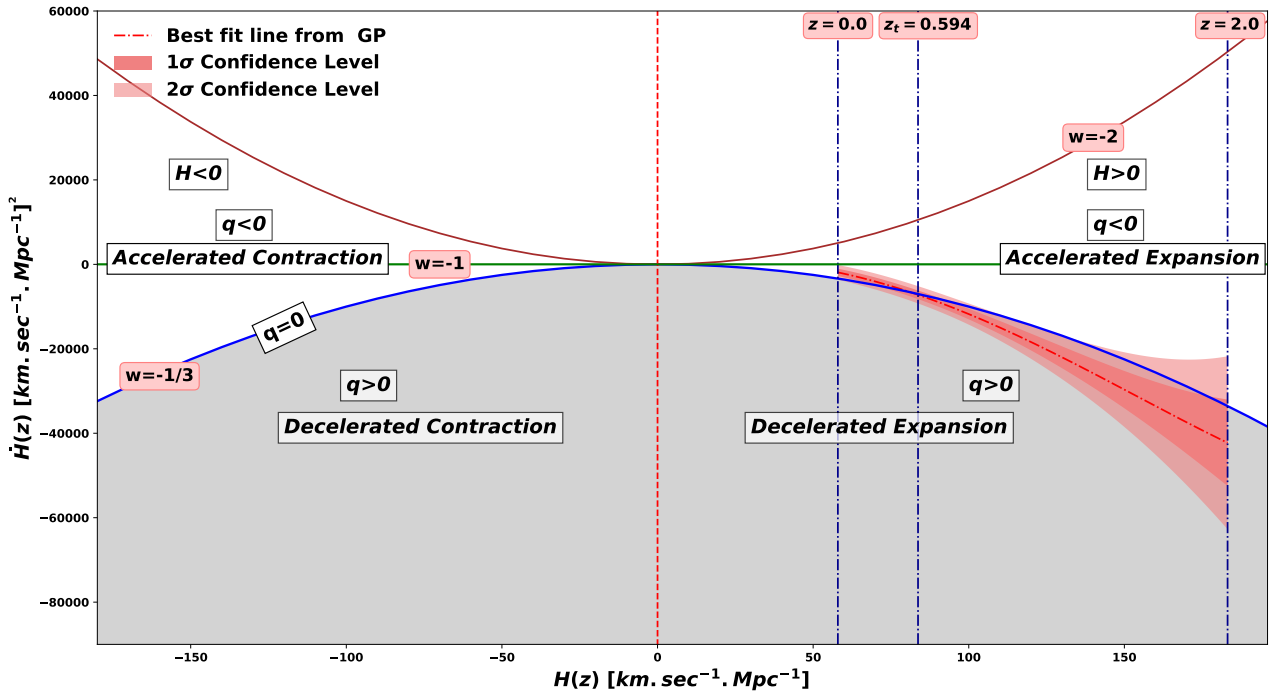


Figure 9. The Hubble Phase Space Portrait reconstructed by using 100 simulated Hubble parameter datapoints.

Rani N., Jain D., Mahajan S., Mukherjee A., Pires N., 2015, *J. Cosmology Astropart. Phys.*, **12**, 045  
 Rapetti D., Allen S. W., Amin M. A., Blandford R. D., 2007, *MNRAS*, **375**, 1510  
 Ratra B., Vogeley M. S., 2008, *PASP*, **120**, 235  
 Ratsimbazafy A. L., Loubser S. I., Crawford S. M., Cress C. M., Bassett B. A., Nichol R. C., Väisänen P., 2017, *MNRAS*, **467**, 3239  
 Riess A. G., et al., 1998, *AJ*, **116**, 1009  
 Riess A. G., et al., 2004, *ApJ*, **607**, 665  
 Riess A. G., et al., 2007, *ApJ*, **659**, 98

Sandage A., 1962, *ApJ*, **136**, 319  
 Scolnic D. M., et al., 2018, *ApJ*, **859**, 101  
 Seikel M., Clarkson C., Smith M., 2012, *J. Cosmology Astropart. Phys.*, **06**, 036  
 Shapiro C., Turner M. S., 2006, *ApJ*, **649**, 563  
 Sharov G. S., Vorontsova E. G., 2014, *J. Cosmology Astropart. Phys.*, **10**, 057  
 Simon J., Verde L., Jimenez R., 2005, *Phys. Rev. D*, **71**, 123001  
 Stern D., Jimenez R., Verde L., Kamionkowski M., Stanford S. A., 2010, *J. Cosmology Astropart. Phys.*, **02**, 008

- Suzuki N., et al., 2012, *ApJ*, 746, 85
- Vargas dos Santos M., Reis R. R. R., Waga I., 2016, *J. Cosmology Astropart. Phys.*, 02, 066
- Velasquez-Toribio A. M., Fabris J. C., 2022, *Brazilian Journal of Physics*, 52, 115
- Velasquez-Toribio A., Magnago A. d. R., 2020, *The European Physical Journal C*, 80, 1
- Wang F. Y., Dai Z. G., 2006, *MNRAS*, 368, 371
- Xu L., Li W., Lu J., 2009, *J. Cosmology Astropart. Phys.*, 07, 031
- Zhang C., Zhang H., Yuan S., Liu S., Zhang T.-J., Sun Y.-C., 2014, *Research in Astronomy and Astrophysics*, 14, 1221

This paper has been typeset from a  $\text{\TeX}/\text{\LaTeX}$  file prepared by the author.